

Dynamical Regimes Induced by Spin Transfer in Magnetic Nanopillars.

Weng Lee Lim, Andrew Higgins, and Sergei Urazhdin
Department of Physics, West Virginia University, Morgantown, WV 26506

We demonstrate the predicted out-of-plane precession induced by spin transfer in magnetic nanostructures with in-plane magnetic field. We show that other magnetic excitations have a significant effect on the stability of the out-of plane precession, making it extremely sensitive to the orientation of the applied magnetic field. The data are supported with micromagnetic simulations. Our results elucidate the relation between the excitation spectrum and the specific dynamical behaviors of nanoscale magnets.

PACS numbers: 85.75.-d, 75.60.Jk, 75.70.Cn

Spin transfer torque (ST) [1] exerted on nanomagnets by spin-polarized current I can induce dynamical states not accessible by any other techniques, providing a unique opportunity to test our understanding of nanomagnetism [2]. At I just above the excitation threshold, ST acting on the magnetic moment m_1 of a nanomagnet F_1 causes precession on an elliptically shaped orbit, determined by a combination of the magnetic field H and the anisotropy of F_1 . The nanomagnet is usually a thin film whose anisotropy is dominated by the demagnetizing field, with H commonly in the film plane. The precession amplitude grows with I , resulting in an orbit known as the clamshell mode (left inset in Fig. 1). Good agreement between calculations and experiments has been achieved for precessional dynamics in this regime [3, 4].

However, fast operation of magnetic devices driven by ST will likely be performed in the less explored high-current regime. According to simulations [4, 5, 6], the extreme points of clamshell eventually merge, resulting in a crossover to the out-of-plane (OP) precession mode consisting of either the lower or the upper half of the clamshell. Only a broad spectral feature indicative of this mode has been seen [3], suggesting that micromagnetic simulations may not be adequate for the highly excited dynamical states of nanomagnets, or that current-induced effects may not be fully described by the established ST mechanisms.

ST also affects the magnetic layer F_2 used to polarize the current, which can decrease the dynamical coherence and suppress the OP mode [7]. Here, we report observation of the OP precession in devices where this effect was minimized by using an extended F_2 . We identified and analyzed the effects of varied direction and magnitude of H . The micromagnetic simulations support our interpretation of the data, and provide insight into the microscopic origins of the observed behaviors. Some of the results could not be reproduced by simulations, suggesting that the understanding of current-induced dynamics in nanomagnets is still incomplete.

Multilayers $\text{Cu}(50)\text{Py}(20)\text{Cu}(5)\text{Py}(5)\text{Au}(20)$, where $\text{Py}=\text{Ni}_{80}\text{Fe}_{20}$ and thicknesses are in nm, were deposited on oxidized silicon at room temperature (RT) by mag-

netron sputtering at base pressure of 5×10^{-9} Torr, in 5 mTorr of purified Ar. $F_1=\text{Py}(5)$ and about 5 nm-thick part of $F_2=\text{Py}(20)$ were patterned by Ar ion milling through an evaporated Al mask with dimensions of $100 \text{ nm} \times 50 \text{ nm}$, followed by deposition of 30 nm of undoped Si without breaking the vacuum. This procedure avoids oxidation of the magnetic layers, which can affect the magnetic dynamics [8]. The mask was removed by a combination of ion milling with Ar beam nearly parallel to the sample surface, and etching in a weak solution of HF in water, followed by sputtering of a 200 nm thick Cu top contact. We discuss data for one of three devices that exhibited similar behaviors.

All measurements were performed at RT. The sample was contacted by coaxial microwave probes, which were connected through a bias tee to a current source, a lock-in amplifier, and a spectrum analyzer through a broadband amplifier. To enable the detection of the precessional states by electronic spectroscopy, H was rotated in the sample plane by angle $\phi = 40^\circ$ with respect to the nanopillar easy axis, unless specified otherwise. Positive I flowed upwards. The device was characterized by magnetoresistive (MR) measurements of its response to H and I , yielding the parameters essential for modeling, such as the MR of 0.21Ω , the dipolar coupling field of 200 Oe caused by the partial patterning of F_2 , and the coercivity of 175 Oe. The latter was consistent with Stoner-Wohlfarth approximation, indicating uniform magnetic reversal. The measured microwave signals were adjusted for the frequency-dependent gain of the amplifier and losses in the cables and probes, determined with a calibrated microwave generator and a power meter.

Fig. 1 shows the dependence of the measured power spectral density (PSD) on H . The spectra at $H = 550$ Oe exhibit three harmonically related peaks at $I < 5$ mA, caused by the clamshell precession. The expected fundamental frequency of the OP mode is close to the frequency of the clamshell's second harmonic near the crossover, since its trajectory is half that of clamshell. The 550 Oe data in Fig. 1 exhibit a spectral feature at $I > 5$ mA consistent with this relationship between the two modes. Below, we present measurements and micro-

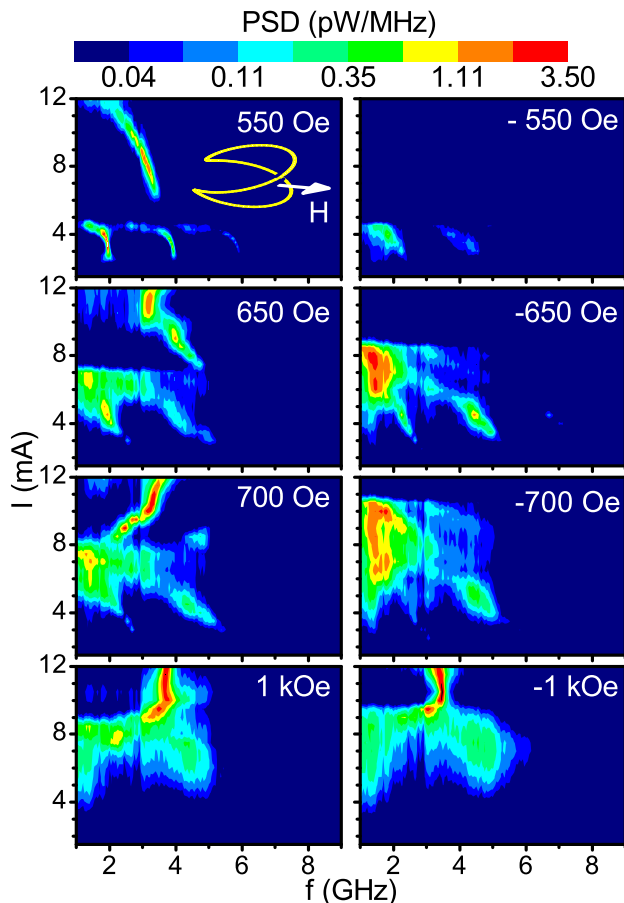


FIG. 1: PSD vs. frequency f and I , at the labeled values of H . The logarithmic data scale brings out a break at 2.93 GHz of about 50 fW/MHz due to the spectrum analyzer crossover. Inset: clamshell trajectory of the magnetic moment, with H shown.

magnetic simulations that confirm our interpretation and elucidate other, more complex dynamical behaviors.

At $H > 550$ Oe, the OP peak rapidly shifts to higher frequency. Simultaneously, the high-current part of the peak splits from the lower part, and eventually merges with the clamshell peaks ($H = 650$ Oe and 700 Oe data in Fig. 1). One can estimate the precession amplitude based on the total microwave power under the peaks divided by I^2 (see also the description of simulations). The largest possible emitted power for hypothetical oscillations between the parallel (P) and antiparallel (AP) configurations of the magnetic layers is 37.7 pW/mA² for our sample. The power generated by clamshell precession at $H = 700$ Oe, $I = 3.5$ mA is 11.2 pW/mA², and by the OP mode at the same H and $I = 10$ mA is 9.9 pW/mA². Both values correspond to the in-plane precession angle exceeding 90°, providing a strong evidence for our interpretation of the spectral peaks as large-angle precessional modes. If these spectral features were induced by inhomogeneous dynamics

rather than precession, they would result in significantly smaller microwave power emission. The first clamshell harmonic exhibits the smallest FWHM of 30 MHz at $H = 550$ Oe, $I = 3.5$ mA. The peaks decrease in amplitude and broaden with increasing H . These behaviors suggest increasingly inhomogeneous dynamics, resulting in decoherence of precession. In contrast, the intensity of the OP peak at $I = 10$ mA increases from 0.86 pW/MHz at $H = 550$ Oe to 2.5 pW/MHz at 1 kOe, while the FWHM remains approximately constant at 140 ± 15 MHz.

The spectra are asymmetric with respect to the direction of H , as illustrated by the difference between the left and the right panels in Fig. 1. The clamshell peaks are consistently broader at $H < 0$ than at $H > 0$. At large I , they are replaced by incoherent noise rather than the OP mode. The direction of H for which the OP mode was observed varied among the samples, indicating extrinsic origin of asymmetry. At large H , the data became similar for positive and negative H . In particular, the $H = \pm 1$ kOe data exhibit a sharp OP peak at $I \geq 9$ mA.

To gain insight into the origin of the behaviors shown in Fig. 1, as a well as other results discussed below, we performed micromagnetic simulations with OOMMF open code software [9]. The simulations included the current-induced ST and Oersted field effects, but neglected thermal fluctuations. The dipolar field was accounted for by subtracting 200 Oe from the in-plane component of H . The cell size was $4 \times 4 \times 5$ nm³. Reducing the size to $2 \times 2 \times 5$ nm³ did not significantly affect the results. The parameter values available mostly from MR measurements [10] were used: current polarization $p = 0.7$, Py exchange stiffness $A = 1.3 \times 10^{-6}$ erg/cm, Gilbert damping $\alpha = 0.03$, and the ratio $\Lambda = 1.3$ of the ST magnitudes near the AP and the P states. Saturation magnetization $M = 750$ emu/cm³ of Py was determined by magnetometry of a Py(5) film prepared under the same conditions as the nanopillar.

The spectra were calculated from the simulated time-dependent magnetization distribution of the nanopillar. The calculated time-dependent resistance was $R(t) = R_0 + \Delta R(t)$, where $R_0 = (R_P + R_{AP})/2$, and $\Delta R(t) = (R_P - R_{AP})\langle \mathbf{s}_1 \cdot \mathbf{s}_2 \rangle / 2$. Here, $\mathbf{s}_1(t), \mathbf{s}_2(t)$ are the local normalized magnetizations of F_1 and F_2 , and $\langle \rangle$ denotes averaging over the simulation grid. The ac voltage on the input of the amplifier $V(t) = \frac{I \Delta R(t)}{1 + R_0 / 50 \Omega}$ was obtained by assuming that a constant current I is distributed between a 50 Ω load and the sample resistance $R(t)$. Fast Fourier transform (FFT) of $V(t)$ over a period of $T = 16.4$ ns with a 1 ps step was performed after relaxation for 10 ns. The power spectral density was determined by $PSD(f) = 2V^2(f)/(50 \Omega \Delta f)$, where $\Delta f = 1/T$, and a factor of 2 accounts for the negative- f contribution to the FFT.

Our calculations showed that a significant asymmetry of spectra with respect to the direction of H can be in-

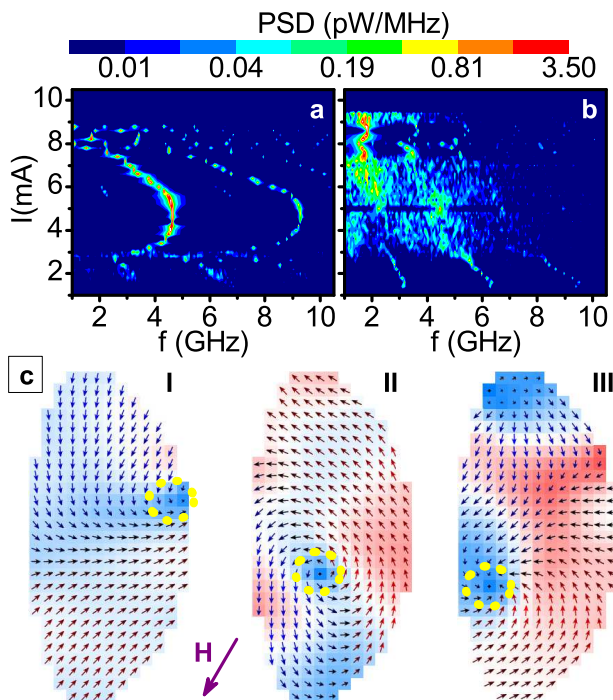


FIG. 2: (a) Calculated PSD for $H = 650$ Oe. (b) same as (a), for $H = -650$ Oe. (c), instantaneous magnetization distribution for $H = -650$ Oe, $I = 6$ mA, captured in the I-II-III sequence with a 100 ps interval, showing the nucleation, propagation, and annihilation of a vortex; the motion of its core is marked with yellow dots. The intensity of blue(red) reflects the out-of-plane component of the magnetization above(below) the plane. Arrow shows the direction of H .

duced by the simultaneous effects of the current-induced Oersted field and a modest asymmetry of the sample geometry. Fig. 2 shows results for a nanopillar approximated by two semi-ellipses with minor semi-axes of 34 nm and 18 nm, and a major axis of 104 nm. Coherent OP precession was obtained at $H > 0$, but was suppressed at $H < 0$ by vortices and finite-wavelength spin-waves [11]. The vortices usually nucleated at the right upper edge of the nanopillar, and annihilated at the lower left edge (Fig. 2c). The chirality of the vortices coincided with the direction of the Oersted field's rotation, indicating that the asymmetry of spectra is caused by the suppression or enhancement of vortex nucleation due to the interplay of sample shape asymmetry and the effect of Oersted field.

Simulations could not reproduce several features of the data for any reasonable variations of nanopillar shape, distribution of current and its polarization, or Py stiffness. Firstly, the simulated OP peak did not exhibit the rapid shift and splitting with increasing H seen in data. Secondly, despite a significant asymmetry of the calculated spectra, they did not reproduce the region at $I > 5$ mA where sharp OP peak was present for $H = 500$ Oe, but no dynamical features appeared at

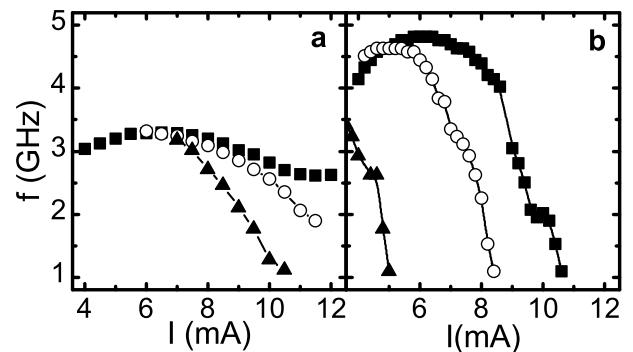


FIG. 3: Frequency of the OP peak *vs* I for $\phi = 48^\circ$ (squares), $\phi = 40^\circ$ (open circles), $\phi = 24^\circ$ (triangles). (a) Measurements performed at $H = 550$ Oe, (b) Calculations performed at $H = 650$ Oe, with the same notations.

$H = -550$ Oe. The simulations also indicated that the OP mode should exhibit multiple spectral harmonics, while only one or two harmonics could be seen in data, regardless of the large amplitude of precession established from the analysis of peak intensity. These features may be caused by additional effects of spin-polarized current neglected by the model, or by the dynamical states not described by micromagnetic simulations.

The differences between data and simulations also open the possibility that the high-current spectral feature in Fig. 1 is caused by dynamics different from the OP mode. Current-induced excitation of the polarizing layer F_2 can lead to microwave peaks, appearing above the onset current determined by the ratio of the volumes of F_2 and F_1 [3]. However, the effective volume of the extended layer F_2 in our samples far exceeds that of F_1 , and thus cannot explain the onset current that at 550 Oe is only 2.6 times larger than the onset of the clamshell precession. The nanopillar shape imperfections can also result in precession around a configuration intermediate between the AP and P states. However, this intermediate state would quickly become unstable at increased H , contrary to the high-field data in Fig. 1. Such a state would also likely appear as an intermediate-resistance step not seen in our dc measurements of MR.

Both measurements and simulations showed that the OP precession is extremely sensitive to the orientation of H , when the latter was rotated in the film plane or tilted out of plane. Rotating H in the plane changed the dependence of the OP mode frequency on I , Fig. 3(a). At $\phi = 48^\circ$, the peak exhibited a blue shift up to 6.5 mA, above which it gradually red shifted. At smaller values of ϕ , the peak broadened, decreased in intensity, and red shifted. The correlation between the width of the OP peak and the dependence of its frequency on I is consistent with published simulations [2, 6]. Namely, blue shift is always predicted in the macrospin approximation, which is more applicable to narrow coherent peaks. In

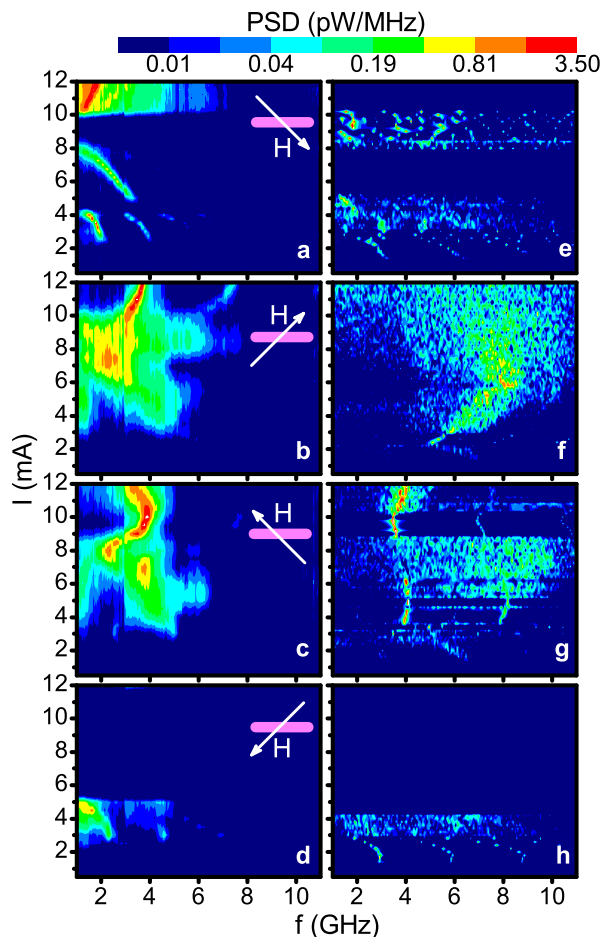


FIG. 4: PSD for $|H| = 900$ Oe tilted by 45° with respect to the sample plane, at $\phi = 40^\circ$. Insets are side view schematics for the orientation of H with respect to the pillars, where positive in-plane direction of H is to the right. (a)-(d) Measurements, (e)-(h) Simulations.

contrast, the peaks can red shift in micromagnetic simulations of the more inhomogeneous dynamics associated with broader spectral peaks. The red shift originates from the decrease of the total magnetic moment of the nanopillar caused by the inhomogeneity. This interpretation was supported by our simulations (Fig. 3(b)), where decreasing ϕ resulted in increasingly inhomogeneous OP dynamics. The OP mode red shifted with I at small ϕ . At larger ϕ , it blue shifted at small I and red shifted at large I , in excellent overall agreement with the data. A somewhat larger H was used in simulations to destabilize the static current-induced AP state at large I (see discussion of Fig. 1).

For H tilted with respect to the sample plane, the dynamics showed dependence not only on the sign of H , but also on its tilting direction (Fig. 4). The component of H perpendicular to the film plane was significantly smaller than the demagnetizing field of 9.4 kOe, resulting in only

5° tilting of m_1 when it was static. The OP mode appeared for both directions of H above the film plane, and was suppressed for H below the film plane. The different response of dynamics to the opposite directions of tilting indicates a significant asymmetry of this state with respect to the film plane. This asymmetry characteristic of the OP dynamics was reproduced by the simulations, as shown in panels (e)-(h). Simulations for H tilted above the sample plane showed predominantly coherent OP precession *below the plane*, in excellent agreement with robust spectral features seen at large I in the data of Figs. 4(b,c). We note that simulations with in-plane H also showed OP precession below the plane, determined by the relative orientations of H and the nanopillar easy axis. In contrast, simulations with H tilted below the sample plane showed OP precession above the sample plane suppressed by dynamical inhomogeneities. These results are consistent with the data.

In summary, coherent current-induced dynamics in magnetic nanopillars was achieved by employing an extended polarizing layer. A high-current spectral peak was identified as the out-of-plane precession, whose dependence on the orientation of H was in excellent agreement with micromagnetic simulations. The dynamics exhibited a significant asymmetry with respect to the direction of H , attributed to a combination of nanopillar shape asymmetry and Oersted field.

This work was supported by the NSF Grant DMR-0747609 and a Cottrell Scholar award from the Research Corporation.

-
- [1] J. Slonczewski, J. Magn. Magn. Mater. **159**, L1 (1996).
 - [2] S.I. Kiselev, J.C. Sankey, I.N. Krivorotov, N.C. Emley, R.J. Schoelkopf, R.A. Buhrman, D.C. Ralph, Nature **425**, 380 (2003).
 - [3] I.N. Krivorotov, D.V. Berkov, N.L. Gorn, N.C. Emley, J.C. Sankey, D.C. Ralph, and R.A. Buhrman, Phys. Rev. **B 72**, 064430 (2007).
 - [4] D.V. Berkov, J. Miltat, J. Magn. Magn. Mater. **320**, 1238 (2008).
 - [5] Z. Li, and S. Zhang, JournalPhys. Rev.B 680244042003.
 - [6] D.V. Berkov and N.L. Gorn, Phys. Rev. **B 72**, 094401 (2005).
 - [7] S. Urazhdin, *arXiv:0802.1560v1* (2008).
 - [8] O. Ozatay, P.G. Gowtham, K.W. Tan, J.C. Read, K.A. Mkhoyan, M.G. Thomas, G.D. Fuchs, P.M. Braganca, E.M. Ryan, K.V. Thadani, J. Silcox, D.C. Ralph, and R.A. Buhrman, Nature Mat. **7**, 567 (2008).
 - [9] M.J. Donahue and D.G. Porter, *OOMMF User's Guide*, NISTIR **6376**, NIST Gaithersburg, MD (1999).
 - [10] J. Bass and W.P. Pratt Jr., J. Phys.: Condens. Matter **19**, 183201 (2007).
 - [11] K.J. Lee, A. Deac, O. Redon, J.P. Nozières, and B. Dieny, Nature Mat. **3**, 877 (2004).